Am J Transl Res 2026;18(2):1214-1220
www.ajtr.org /ISSN:1943-8141/AJTR0166506

Case Report

Clinical significance of the outside-stent flow sign in vertebrobasilar dolichoectasia

Zhihua Du[1*], Zhongkui Wang[2*], Rongju Zhang[1*], Xiangyu Cao[1], Xinfeng Liu[1], Bin Lv[1], Baomin Li[1], Jun Wang[1]

[1]Department of Neurology, First Medical Center of PLA General Hospital, Beijing 100853, China; [2]Department of Neurology, Shanghai Deji Hospital, Shanghai 200331, China. [*]Equal contributors.

Received June 1, 2025; Accepted December 11, 2025; Epub February 15, 2026; Published February 28, 2026

Abstract: Vertebrobasilar dolichoectasia (VBD) is a rare, progressive disorder characterized by significant expansion, elongation, and tortuosity of the vertebrobasilar arteries. This case series introduces a novel imaging sign observed in three patients with clinical manifestations of VBD. The presence of outside-stent flow (OSF) may serve as a potential predictor for aneurysm recurrence in VBD following endovascular intervention. Furthermore, OSF could indicate the need for embolization of the contralateral vertebral artery after stenting, with or without coil embolization, in patients with VBD aneurysms.

Keywords: Vertebrobasilar dolichoectasia, outside-stent flow, sign, recurrence

Introduction

Vertebrobasilar dolichoectasia (VBD) is a progressive disorder marked by dilation, elongation, and tortuosity of the vertebrobasilar (VB) arteries [1], which can result in a range of symptoms, including ischemic stroke, brainstem and cranial nerve compression, and intracranial hemorrhage [2]. The etiology and pathogenesis of VBD remain unknown.

Due to its complex morphology and the absence of randomized studies or clear treatment guidelines, management of VBD remains controversial and challenging [3]. While endovascular interventional treatments (EVT), such as flow diversion, overlapping stents, and coil-assisted stent reconstruction, show promise, recurrence of aneurysms in VBD has been reported after such interventions [3], necessitating evaluation of the risk of recanalization. Therefore, an imaging marker to identify factors predisposing to VBD recurrence is essential.

Outside-stent flow (OSF) refers to the continuous blood flow or significant stagnation outside the stent wall. Following stent deployment from the basilar artery (BA) to a vertebral artery (VA), the stent obstructs blood flow in the contralateral VA, resulting in OSF, which may influence the effectiveness of EVT in VBD patients. A review of the literature search revealed no previous reports or did not identify publications specifically examining OSF. This study presents our single-center experience with the predictive value of OSF for VBD recurrence.

Case presentation

Case 1

A 58-year-old male with a history of hypertension presented to the neurology emergency department with sudden-onset vertigo and gait disturbance. Cerebral magnetic resonance imaging (MRI) revealed long T1 and T2 signals, along with high signals on diffusion-weighted imaging (DWI) in the left pons. Cerebral angiography showed dilated and tortuous distal right VA (RVA) and proximal to middle BA in the prepontine and premedullary cisterns (**Figure 1A**, **1B**). The maximum BA diameter was 9.29 mm.

Dual antiplatelet therapy, consisting of aspirin (100 mg/day) and ticagrelor (45 mg twice daily), was initiated four days prior to stenting. Two LEO stents (5.5 mm × 75 mm; Balt Extrusion, Montmorency, France) were deployed in series

https://doi.org/10.62347/WSKG8585

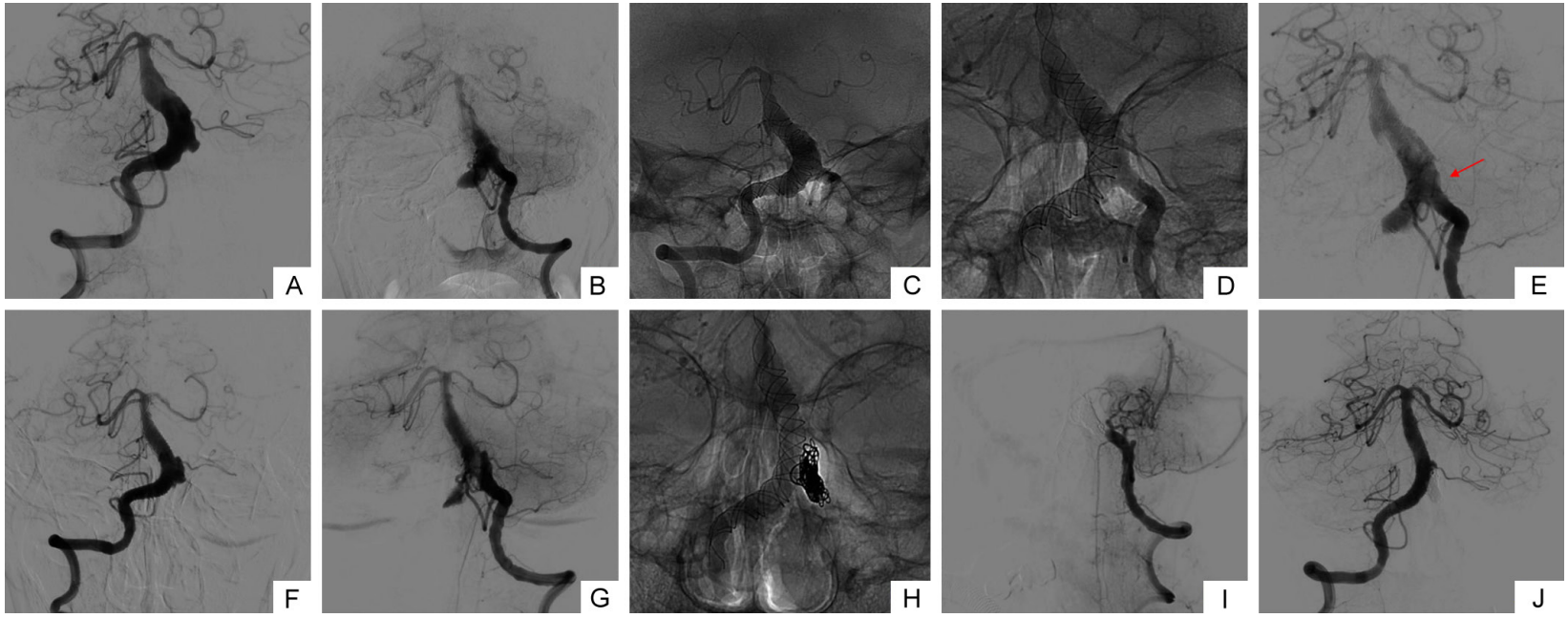

Figure 1. Case 1. A, B. Angiographic images from the front view showing the dilated and tortuous distal right vertebral artery (VA) and the proximal and middle basilar artery (BA). C, D. Angiography of the right VA after implantation of two LEO stents (5.5 mm × 75 mm) in the BA and right VA. E. Angiography of the left VA showing outside-stent flow (OSF) on the left side of the vertebrobasilar junction (red arrow). F. Six-month angiographic follow-up showing complete reconstruction of the BA and right VA. G. Left vertebral angiography revealing a significant increase in OSF on the left side of the stents. H. Image without bone subtraction showing coil embolization with occlusion at the V4 portion of the left VA. I. Left vertebral angiography after embolization showing no blood flow within the coil mass. J. Twelve-month angiographic follow-up demonstrating full reconstruction of the BA without aneurysm recanalization and complete elimination of OSF.

along the BA and RVA using the standard telescopic technique with ~30% overlap (**Figure 1C**, **1D**). Immediate left VA (LVA) angiography revealed OSF at the left VB junction (**Figure 1E**, red arrow). The first angiographic follow-up was performed six months after the procedure. Digital subtraction angiography (DSA) demonstrated persistence of vertebrobasilar dolichoectasia (VBD) without evidence of repair. RVA angiography demonstrated that the parent artery walls were well reconstructed by the telescoping stents (**Figure 1F**). LVA angiography showed a significant increase in OSF at the left VB junction (**Figure 1G**). To prevent aneurysm expansion, LVA embolization was performed using steel coils. A 6-French Envoy guiding catheter (Cordis, Johnson & Johnson, Miami, FL, USA) was advanced over a 0.035-inch soft glidewire into the V2 portion of the LVA. An Echelon-10 microcatheter was introduced through the guiding catheter into the V4 portion of the LVA using a Synchro-14 micro-guidewire. Five coils were deployed through the microcatheter as close as possible to the LEO stents until angiographic extravasation was no longer evident (**Figure 1H**, **1I**). Angiographic follow-up at 12 months showed complete VB artery reconstruction and full resolution of OSF (**Figure 1J**).

Case 2

A 22-year-old man with no significant medical history presented to our hospital with a progressive headache that had persisted for two months. Cerebral angiography revealed a dilated and tortuous proximal and middle BA (**Figure 2A**). The maximum BA diameter was 12.92 mm. Based on these findings, endovascular treatment (EVT) was initiated. Standard antiplatelet therapy with aspirin and clopidogrel was started five days prior to stenting. A 6-French guiding catheter was introduced through a femoral sheath into the V2 segment of the RVA. The Echelon-10 microcatheter was initially placed within the aneurysm lumen to deliver coils. A Vasco microcatheter was advanced into the left posterior cerebral artery, and two overlapping LEO stents (5.5 × 75 mm and 5.5 × 40 mm) were deployed at its end, ensuring two layers of metal coverage across the BA and RVA. Four Axuim coils (Medtronic PLC) were subsequently delivered into the aneurysm *via* the Echelon-10 microcatheter (**Figure 2B**). Immediate left vertebral (LV) angiography revealed partial occlusion of the dissecting aneurysm of the BA (**Figure 2C**) and notable OSF on the left side of the stents (**Figure 2D**, **2E**, red arrow). At twelve months, DSA indicated a marked rise in OSF supplying the right posterior inferior cerebellar artery (PICA) on the left side of the telescoping stents, confirming VBD recurrence on follow-up (**Figure 2F-H**). Immediate embolization of the LVA was performed using steel coils (**Figure 2I**). At the three-month postoperative DSA *via* RVA, complete occlusion of the basilar dissecting aneurysm was observed, with no signs of OSF or right PICA occlusion (**Figure 2J**).

Case 3

A 38-year-old man with no significant medical history was admitted to our hospital following the onset of vertigo. Angiographic imaging revealed a fusiform aneurysmal dilatation of the tortuous BA (**Figure 3A**), with a maximum diameter of 8.55 mm. The patient started daily oral aspirin (100 mg) and clopidogrel (75 mg) for seven days and was scheduled for stent-assisted coil embolization. Two LEO stents (4.5 mm × 50 mm) were deployed in the BA and RVA using the standard telescopic technique (**Figure 3B**, **3C**). Subsequently, an Echelon-14 microcatheter was advanced into the stent lumen and through the stent struts into the BA aneurysm with a guidewire. The aneurysm was partially embolized with three detachable coils. DSA revealed significant OSF to the left inferior anterior cerebellar artery on the left side of the LEO stents (**Figure 3D**, red arrow). A 6-French guiding catheter was then advanced to the distal LVA, and the Echelon-14 microcatheter was positioned in the V4 segment of the LVA. Endovascular embolization of the LVA was performed using two steel coils (**Figure 3E**, **3F**).

Computational fluid dynamics (CFD) analysis was employed to assess wall shear stress (WSS) in the parent artery, predicting the effect of OSF on recanalization of VBD after endovascular embolization. Three-dimensional DSA was performed to obtain raw data, which were reconstructed using Mimics 17 (Materialise, Leuven, Belgium) to create STL files. The STL files were subsequently processed in Geomagic Studio 12.0 (Geomagic, Research Triangle Park, North Carolina) for model repairing, trimming, and smoothing, yielding models for finite

Figure 2. Case 2. A. Angiography of the right vertebral artery (VA) showing a tortuous and dilated proximal and middle basilar artery (BA). B. Image without bone subtraction showing deployment of two LEO stents (5.5 mm × 75 mm and 5.5 mm × 40 mm) and insertion of four coils under stent protection. C. Angiography of the right VA revealing partial occlusion of the dissecting aneurysm of the BA. D, E. Angiography in both front and lateral views of the left VA showing notable outside-stent flow (OSF) on the left side of the LEO stents (red arrow). F-H. Twelve-month angiographic follow-up demonstrating a remarkable increase in OSF supplying the right posterior inferior cerebellar artery (PICA). I. Image without bone subtraction showing coil embolization with occlusion of the left VA. J. Fifteen-month angiographic follow-up showing complete occlusion of the basilar dissecting aneurysm with no sign of OSF.

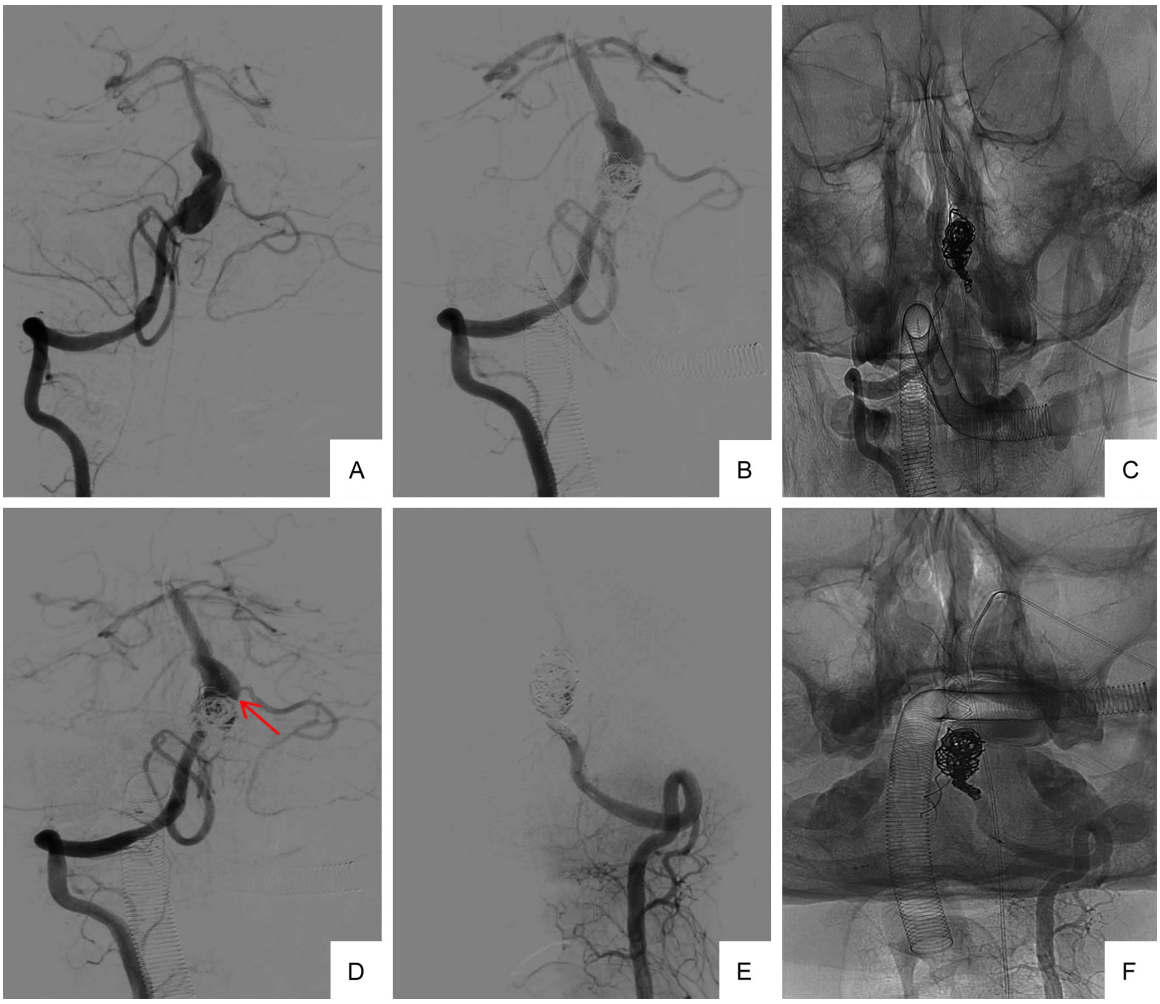

Figure 3. Case 3. A. Angiography of the right vertebral artery (VA) showing fusiform aneurysmal dilatation of the basilar artery (BA). B, C. LEO stent-assisted coil embolization with two LEO stents (4.5 mm × 50 mm) using the standard telescopic technique (unsubtracted view) with partial aneurysm occlusion. D. Angiography of the right VA revealing significant OSF on the left side of the LEO stents. E, F. Complete coil embolization of the left vertebral artery.

element and fluid dynamics simulations. The virtual treatment model then underwent fluid dynamics analysis. The vascular and post-deployment stent models were imported into ICEM 16.2 (Ansys, Canonsburg, PA) for mesh generation, and simulations were performed using the Navier-Stokes equations under steady-state assumptions. These were imported into Geomagic Studio 12.0 (Geomagic, Research Triangle Park, NC) for repair, trimming, and smoothing to generate a model for subsequent finite element and hydrodynamic simulations. A LEO stent model was created in SolidWorks (Dassault Systems, SolidWorks Corp., MA) based on geometric specifications. The virtual model was subjected to hydrodynamic simulation in ICEM 16.2 (Ansys, Canonsburg, PA) to generate mesh files. Hemodynamic simulations followed the Navier-Stokes equations for steady-state analysis. WSS was calculated using Poiseuille's law with the following formula [4]: WSS = 4 × η × Vm/inner diameter (dyne/cm^2).

In this formula, η is blood viscosity, and Vm is mean blood flow velocity.

Before stent placement, the BA aneurysm showed low WSS distribution (**Figure 4A1-C1**). After the first LEO stent was implanted, there was an increase in WSS (1.79 Pa) (**Figure 4A2-C2**), and a further increase in WSS (1.97 Pa) with elevated flow velocity at the left proximal BA after deployment of the second LEO

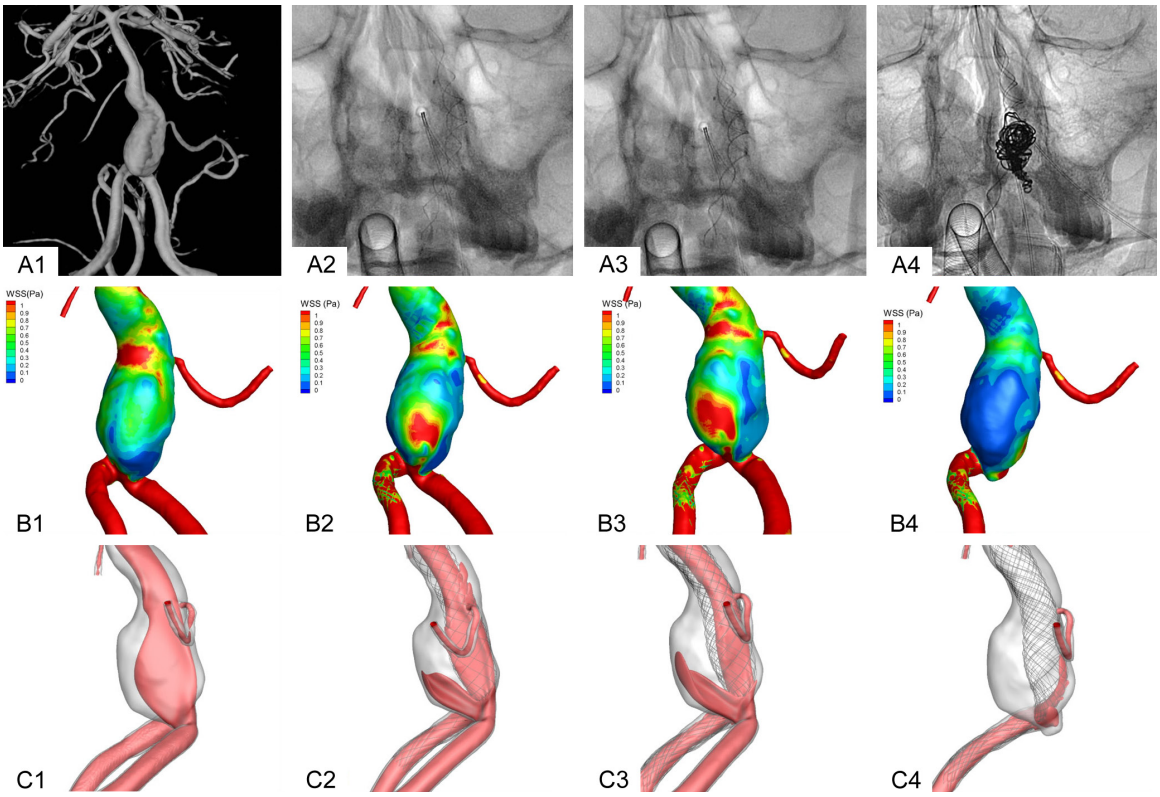

Figure 4. Case 3: Computational fluid dynamics (CFD) simulations. Wall shear stress (WSS) simulations of the aneurysm in: (A1-C1) No LEO stent implantation, (A2-C2) After implantation of one LEO stent, (A3-C3) After implantation of two LEO stents, and (A4-C4) After implantation of two LEO stents with embolization of the left vertebral artery.

stent (**Figure 4A3-C3**). Following LVA embolization, fluid velocity and WSS decreased significantly to 0.11 Pa (**Figure 4A4-C4**).

Discussion

The BA is the most complex hemodynamic vessel in the cerebral circulation, and the occurrence and progression of VBD are closely linked to hemodynamic factors. Therefore, blood flow reconstruction plays a critical role in the treatment of VBD.

Currently, stenting reconstruction and stent-assisted coil embolization, based on aneurysm morphology, are the preferred EVTs for VBD. Stenting can reduce the size of the VBD aneurysm, thereby alleviating mass effects associated with VBD. However, EVTs carry a high operative risk and complication rate, with incidence estimates ranging from 10.5% to 22.2% [5, 6]. Consequently, careful manipulation during the EVT procedure is essential.

Previous studies have indicated that hemodynamic factors are key in clinical treatment and in evaluating the therapeutic outcomes of aneurysms [7, 8]. For occlusion, regions of high WSS and increased blood flow velocity within the aneurysm lumen after EVT are considered risk factors for aneurysm recurrence [9]. Frösen [10] demonstrated that cerebral blood flow leading to high WSS contributes to intracranial aneurysm formation and induces wall remodeling. However, the relationship between WSS and VBD remains underexplored. In this study, case 1 and case 2 illustrate the clinical progression and imaging findings of OSF immediately following stenting of the VB artery in VBD patients. OSF was consistently observed near the VB junction, a region prone to future recanalization, suggesting that OSF may play a significant role in aneurysm recurrence after EVT.

Virtual treatment techniques that combine finite element and CFD simulations offer a valuable tool for exploring the mechanisms underly-

ing EVT modalities [11]. Simulating the treatment of case 3 revealed that stent implantation hindered the merging of blood flow from the RVA and LVA, leading to blood flow from the RVA into the aneurysm and creating a high-flow region within the aneurysm lumen. WSS on the aneurysm surface increased as the number of stents increased. The stent obstruction impeded smooth blood flow along the BA, resulting in continuous pressure buildup within the aneurysm lumen. This pressure increase is a key factor contributing to aneurysm and branch vessel expansion. Notably, WSS decreased significantly after LVA occlusion, and the OSF signs disappeared.

To our knowledge, this study is the first to evaluate the predictive value of OSF for aneurysm recurrence after EVT in VBD. OSF following stenting with or without coil embolization in VBD patients is an important indicator for embolization of the contralateral VA. Further research is needed to fully evaluate the efficacy of the OSF sign in predicting aneurysm recurrence in VBD after EVT.

Disclosure of conflict of interest

None.

Address correspondence to: Dr. Jun Wang, Department of Neurology, First Medical Center of PLA General Hospital, Beijing 100853, China. E-mail: wangjun301@126.com

References

[1] Passero SG and Rossi S. Natural history of vertebrobasilar dolichoectasia. Neurology 2008; 70: 66-72.

[2] Shapiro M, Becske T, Riina HA, Raz E, Zumofen D and Nelson PK. Non-saccular vertebrobasilar aneurysms and dolichoectasia: a systematic literature review. J Neurointerv Surg 2014; 6: 389-393.

[3] Wang Y and Yu J. Prospects and dilemmas of endovascular treatment for vertebrobasilar dolichoectasia. Front Neurol 2022; 5: 895527.

[4] Wang C, Chen M, Liu SL, Liu Y, Jin JM and Zhang YH. Spatia distribution of wall shear stress in common carotid artery by color Doppler flow imaging. J Digit Imaging 2013; 26: 466-471.

[5] Wu X, Xu Y, Hong B, Zhao WY, Huang QH and Liu JM. Endovascular reconstruction for treatment of vertebrobasilar dolichoectasia: long-term outcomes. Am J Neuroradiol 2013; 34: 583-588.

[6] He X, Duan C, Zhang J, Li X, Zhang X and Li Z. The safety and efficacy of using large woven stents to treat vertebrobasilar dolichoectasia. J Neurointerv Surg 2019; 11: 1162-1166.

[7] Sindeev S, Arnold PG, Frolov S, Prothmann S, Liepsch D, Balasso A, Berg P, Kaczmarz S and Kirschke JS. Phase-contrast MRI versus numerical simulation to quantify hemodynamical changes in cerebral aneurysms after flow diverter treatment. PLoS One 2018; 13: e0190696.

[8] Zhang H, Li L, Miao F, Yu J, Zhou B and Pan Y. Computational fluid dynamics analysis of intracranial aneurysms treated with flow diverters: a case report. Neurochirurgie 2022; 68: 235-238.

[9] Luo B, Yang X, Wang S, Li H, Chen J, Yu H, Zhang Y, Zhang Y, Mu S, Liu Z and Ding G. High shear stress and flow velocity in partially occluded aneurys prone to recanalization. Stroke 2011; 42: 745-753.

[10] Frösen J, Cebral J, Robertson AM and Aoki T. Flow-induced, inflammation-mediated arterial wall remodeling in the formation and progression of intracranial aneurysms. Neurosurg Focus 2019; 47: E21.

[11] Perera R, Isoda H, Ishiguro K, Mizuno T, Takehara Y, Terada M, Tanoi C, Naito T, Sakahara H, Hiramatsu H, Namba H, Izumi T, Wakabayashi T, Kosugi T, Onishi Y, Alley M, Komori Y, Ikeda M and Naganawa S. Assessing the risk of intracranial aneurysm rupture using morphological and hemodynamic biomarkers evaluated from magnetic resonance fluid dynamics and computational fluid dynamics. Magn Reson Med Sci 2020; 19: 333-344.